European Conference on Computational Fluid Dynamics
ECCOMAS CFD 2006
P. Wesseling, E. Oñate and J. Périaux (Eds)

NON-UPWIND DISCONTINUOUS-GALERKIN SCHEMES FOR HYPERBOLIC CONSERVATION LAWS IN POROUS MEDIA

Sadok Lamine* **and Michael G. Edwards** †

*University of Wales Swansea, Civil and Computational Engineering Centre
Singleton Park, SA3 4JZ, United Kingdom
e-mail: sadok.lamine@gmail.com

Key words: Non upwind Schemes, Discontinuous Galerkin method, MUSCL schemes, Monotonicity, Gravity driven flows

Abstract. *Discontinuous-Galerkin schemes are presented for convective flow approximation in reservoir simulation. The methods are compared with slope limited MUSCL and TVD schemes.*

Standard reservoir simulation schemes employ single-point upstream weighting (first order upwind) for approximation of the convective fluxes when multiple phases or components are present. Higher order upwind approximations have also been developed, including higher order Godunov schemes. These schemes require a characteristic decomposition when applied to hyperbolic systems with multiple phases or components present. The decomposition leads to optimal upwind schemes where upwind directions are resolved according to characteristic wave components. However the decomposition adds further complexity and additional computation is required to account for the decomposition matrices.

This paper presents novel Discontinuous-Galerkin schemes for reservoir simulation that permit reconstruction of stable higher order monotonicity preserving approximations while avoiding dependence upon both upwinding and characteristic decomposition. The schemes are formulated within a locally conservative finite volume framework.

Results are presented for gravity driven flows, where the wave direction changes sign (reverse flow). Results obtained with the new schemes indicate a competitive comparison with the other higher order schemes.

1 INTRODUCTION

Standard reservoir simulation schemes employ single-point upstream weighting[14] (first order upwind scheme) for approximation of the convective fluxes when multiple phases or components are present. The aim here is to devise robust, accurate, and efficient methods that are entropy satisfying and free of spurious oscillations.

Higher order upwind approximations have been developed for two phase flow multicomponent flow, including higher order Godunov schemes[15,16]. These schemes require a characteristic decomposition when applied to hyperbolic systems modeling a multicomponent multiphase flow. The decomposition leads to optimal upwind schemes where upwind directions are resolved according to characteristic wave components. However the decomposition adds further complexity and additional computation is required to account for the decomposition matrices[12,18]. Componentwise limiting is faster than characteristic limiting and implementation is much simpler for coupled multicomponent multiphase systems.

The discontinuous galerkin (DG) method has been shown to be very attractive for compact higher order approximation of hyperbolic conservation laws[3,4,5,17]. The method is locally conservative and considered to be a generalisation of finite volume methods. The idea converts numerical fluxes with slope limiters into the finite element framework in a very natural way. They are able to capture the entropy satisfying discontinuities without producing spurious oscillations. While the DG approximate solution itself may not be monotonic, the averages on the control volumes, are proven to be monotonicity preserving[3]. Upwind Discontinuous Galerkin (DG) has be is shown to be an efficient method for hyperbolic laws in compositional modeling compared to first order finite difference methods[17].

This paper presents novel locally conservative non upwind DG schemes for reservoir simulation that permit reconstruction of stable higher order monotonicity preserving approximations while avoiding dependence upon both upwinding and characteristic decomposition. The schemes are formulated within a locally conservative finite volume framework. Comparison between the new non upwind schemes and non upwind high order MUSCL (Monotone Upstream Centered Scheme for Conservation Laws)[18] methods is presented. In this paper, we restrict our study to the one space dimension case. Application of RKDG to multidimensional results is the subject of current research.

2 FLOW EQUATIONS

Without loss of generality in terms of the numerical methods applicability, the schemes presented here are illustrated with respect to two phase flow and three component two phase flow models, with unit porosity and where the capillary pressure and dispersion are neglected.

2.1 Two phase flow

We consider a water-oil two phase flow model. In the following, phase quantities bear suffices a for the aqueous phase (water) and o for the oil phase. The conservation equations for a two phase flow, in the absence of source and sink terms, over the domain Ω are written as

$$\int_\Omega \frac{\partial S}{\partial t} + \int_\Omega \frac{\partial V_a}{\partial x} = 0 \tag{1}$$

where S denotes the aqueous phase saturation and V_a is the phase velocity defined via Darcy's law by

$$V_a = -\lambda_a K \frac{\partial \phi}{\partial x} + \rho_a g \frac{\partial h}{\partial x}. \tag{2}$$

Here, λ_a and λ_o are the phase mobilities, K is the medium permeability, ρ is the phase density and h is the altitude of the reservoir. The saturation of the oil phase is deduced from the volume balance equation, where saturations sum to one.
Expressing the phase velocity in terms of total velocity $V_T = V_a + V_o$ as

$$V_a = f(S)(V_T - \lambda_o \Delta\rho g \frac{\partial h}{\partial x}), \tag{3}$$

where f is the fractional flow, the incompressible flow condition, in 1-D, reduces to

$$\frac{\partial V_t}{\partial x} = 0, \tag{4}$$

from which it follows that the total velocity is spatially constant in 1-D for an incompressible flow. Equations (3) and (4) are used to determine pressure and velocity.
Boundary conditions involve specifying initial saturation field with saturation specified at an injection well, here the pressure is specified at the production well.
Further details of flow equations are described in[14].

2.2 Three component flow

The system considered here is comprised of an aqueous phase (water and polymer concentration) together with an oil phase. Define C to be the component concentration in the miscible phase. The conservation equation over Ω in the absence of source and sink terms writes as

$$\int_\Omega \frac{\partial \mathbf{S}}{\partial t} + \int_\Omega \frac{\partial \mathbf{F(S)}}{\partial x} = \mathbf{0}, \tag{5}$$

subject to initial boundary conditions, where $\mathbf{S} = (S, SC)^T$ denote the vector of conservative variables and $\mathbf{F}(\mathbf{S}) = (V_a, CV_a)$ is the nonlinear flux vector, $\mathbf{C} = (S, C)^T$ denotes the vector primitive variables.. The phase velocity is defined by equations (2) and (3).

3 LOCALLY CONSERVATIVE FIRST ORDER APPROXIMATION

We consider schemes in one dimension on $\Omega = [0, 1]$ with discrete nodes $x_j = j\Delta x$ and time $t^n = n\Delta t$. Defining $x_{j+1/2} = \frac{x_j + x_{j+1}}{2}$, $\{I_j\}_{j=1..N}$ with $I_j = (x_{j-1/2}, x_{j+1/2})$ form an equidistant partition of Ω.

Before moving to systems we briefly recall that for a scalar equation of the form

$$\frac{\partial S}{\partial t} + \frac{\partial f(S)}{\partial x} = 0, \tag{6}$$

subject to initial boundary data.

3.1 Locally conservative upwind approximation

The standard explicit first order upwind scheme can be written as

$$S_j^{n+1} = S_j^n - \frac{\Delta t}{\Delta x}(f_{j+1/2}^n - f_{j-1/2}^n) \tag{7}$$

where the approximate flux is defined by

$$f_{j+1/2}^n = \frac{1}{2}[(f_{j+1}^n + f_j^n) - \mid \lambda_{j+1/2} \mid (S_{j+1}^n - S_j^n)] \tag{8}$$

where

$$\lambda_{j+1/2} = \begin{cases} \frac{f_{j+1}-f_j}{S_{j+1}-S_j}, & \mid S_{j+1} - S_j \mid \geq \epsilon; \\ \frac{\partial f}{\partial S}, & \mid S_{j+1} - S_j \mid \leq \epsilon. \end{cases} \tag{9}$$

This definition of wave speed ensures that shocks are captured with precision for any finite jump in S_j with $\lambda_{j+1/2}$ assuming the Rankine-Hugoniot shock speed across a mesh interval. In this form the first order scheme appears as a central scheme and is comprised of a central difference in flux with a central difference of a specific diffusion term. The scheme can be seen in its original upwind form by noting that for a positive wave speed the flux uses data to the left and reduces to $f_{j+1/2} = f(S_j)$, otherwise $f_{j+1/2} = f(S_{j+1})$ and the flux uses data to the right as with single point upstream weighting. While the definition of equations (7), (8) does not require any explicit sign dependence in the scheme, the upwind directions are clearly detected. This explicit scheme is the most fundamental scheme for scalar conservation laws in one dimension and is stable, locally conservative and monotonicity preserving subject to a maximum CFL condition of unity. This scheme requires an entropy fix to disperse expansion shocks[10].

3.2 Systems of hyperbolic equations

In order to apply such a scheme to a system of hyperbolic conservation laws, the system is first decomposed into characteristic form. Decomposition is performed via the transformation

$$\Delta \mathbf{S} = R \Delta W \tag{10}$$

where R is the matrix of right eigenvalues of the system Jacobian Matrix $A = \frac{\partial \mathbf{F}}{\partial \mathbf{S}}$ and the matrix of eigen values Λ is defined via

$$\Lambda = R^{-1} A R \tag{11}$$

and $\Delta \mathbf{S}$, $\Delta \mathbf{W}$ represent the respective conservative and characteristic variable increments. The upwind scheme is in effect applied to each characteristic wave component and the discrete system is recomposed into a conservative form. The first order scheme for a system can be written as

$$\mathbf{S}_j^{n+1} = \mathbf{S}_j^n - \frac{\Delta t}{\Delta x}(\mathbf{f}_{j+1/2}^n - \mathbf{f}_{j-1/2}^n) \tag{12}$$

where the approximate flux is defined by

$$\mathbf{f}^n_{j+1/2} = \frac{1}{2}[(\mathbf{f}^n_{j+1} + \mathbf{f}^n_j) - R \mid \Lambda_{j+1/2} \mid R^{-1}(\mathbf{S}^n_{j+1} - \mathbf{S}^n_j)] \tag{13}$$

provided the definition of discrete eigenvalues $\Lambda_{j+1/2}$ have an appropriate generalization of equation (8) such that conservation and exact shock speed are maintained. The CFL condition now applies with respect to the maximum eigenvalue of the system. The appearance of the matrix of eigenvalues $R_{j+1/2}$ in the system flux approximation is a consequence of characteristic component upwinding. This leads to an optimal diffusive operator in terms of numerical diffusion provided the shock jump criteria can be satisfied for the system in hand.

4 LOCALLY CONSERVATIVE NON UPWIND SCHEMES (1-D)

4.1 Lax Friedrichs Flux

A well known scheme for systems that is monotonicity preserving and has no sign independence is due to Lax and Friedrichs, and takes the form

$$\mathbf{f}_{j+1/2} = \frac{1}{2}[(\mathbf{f}(\mathbf{S}_L) + \mathbf{f}(\mathbf{S}_R)) - \frac{\Delta x}{\Delta t}(\mathbf{S}_R - \mathbf{S}_L)] \tag{14}$$

where S_L and S_R denote the left and right states at the cell interface. In practice, this scheme is too diffusive. This is due to the extra large coefficient of numerical diffusion that corresponds to a CFL of unity.

4.2 Rusanov Flux[11]

A less diffusive scheme of this type can be constructed by noting that if the matrix of eigenvalues R is proportional to the unit matrix then the dependency of the discrete flux on the matrix of eigenvalues is removed, leaving a much simpler coefficient of artificial diffusion. Independence from a characteristic decomposition can be achieved by replacing $\mid \Lambda_{j+1/2} \mid$ with $\mid \Lambda_{RUj+1/2} \mid$ where

$$\mid \Lambda_{RUj+1/2} \mid = \max_{[\mathbf{S}_L, \mathbf{S}_R]} \max_k \mid \lambda^k_{j+1/2}(\mathbf{S}) \mid \mathbf{I} \tag{15}$$

where the maximum absolute eigenvalue of the system over the interval of states $\mathbf{S}$ in $[\mathbf{S}_L, \mathbf{S}_R]$ is used and multiplies the identity matrix. The maximum over the interval also ensures that the entropy condition is satisfied by the Rusanov flux. For the system considered here

$$\mid \Lambda_{RUj+1/2} \mid = \max_{[\mathbf{S}_L, \mathbf{S}_R]} \{\mid \frac{\partial V_a}{\partial S} \mid, \mid \frac{V_a}{S} \mid\} \mathbf{I} \tag{16}$$

The discrete flux takes the form

$$\mathbf{f}_{j+1/2} = \frac{1}{2}[(\mathbf{f}(\mathbf{S}_L) + \mathbf{f}(\mathbf{S}_R)) - \mid \Lambda_{RUj+1/2} \mid (\mathbf{S}_R - \mathbf{S}_L)] \tag{17}$$

The flux of equation (17) is a Local Lax Friedrichs (LLF) based flux[18] based on Liu and Osher in[12] for the Euler Equations.

Since the modulus of each eigenvalue in the diffusion operator is replaced by the maximum absolute eigenvalue over the system and local interval, it follows that the price to pay for this simplification is extra numerical diffusion when compared to characteristic upwinding for a system. However, the Rusanov flux is always less diffusive than the original Lax Friedrichs scheme since the original scheme is based on a uniformly maximum coefficient of diffusion which effectively corresponds to having a unit CFL in the coefficient of numerical diffusion.

5 HIGH ORDER GODUNOV TYPE FINITE VOLUME SCHEMES in 1-D

A significant step in the generalization of Godunov's finite volume method to high order accuracy is due to van Leer[13]. Godunov's method is generalized by employing linear solution reconstruction in each cell. The basic idea in Godunov's method is to treat the averages over the interval, I_j as the basic unknowns and solve the approximate problem exactly. The process of constructing a high order finite volume method is summarized below:

1. **Data reconstruction**: using information from the I_j, higher order piecewise polynomials are reconstructed in each interval. Slope limiters are applied to the higher order data to enforce a local maximum principle and prevent spurious oscillation .

2. **Flux evaluation at the interface**: An entropy satisfying flux is used to resolve the approximate solution of the Riemann problem.

3. **Time evolution**: The favored approach to time accuracy is maintained here via the use of the Rung Kutta method[7], although this would be very expensive for practical reservoir simulation.

When using the discrete Rusanov flux stated in (17), the extension to high order accuracy is simpler to achieve since the non-upwind system formulations have no dependency upon characteristic variables in this definition of flux. The only spectral pieces of information needed are modulus of the local highest characteristic wave speeds. For our case,

$$\Lambda_{RUj+1/2} = \max_{[S_L,S_R]} \{ | \frac{\partial V_a}{\partial S} |, | \frac{V_a}{S} | \} \mathbf{I}. \tag{18}$$

Consequently, a higher order approximation can be introduced for the left and right states respectively and be expressed directly in terms of the conservative variables (componentwise). In this paper, both conservative and primitive variables are compared.

5.1 Data reconstruction

First, the higher order left and right states are defined using a MUSCL formalism [13].

5.1.1 Conservative variables

The componentwise higher order reconstruction is written as

$$\mathbf{S}_L = \mathbf{S}_j + \frac{1}{2}\Phi(\mathbf{r}^+_{j+1/2})(\mathbf{S}_{j+1} - \mathbf{S}_j), \tag{19}$$

$$\mathbf{S}_R = \mathbf{S}_{j+1} - \frac{1}{2}\Phi(\mathbf{r}^-_{j+1/2})(\mathbf{S}_{j+1} - \mathbf{S}_j); \tag{20}$$

where $\Phi(r^{\pm}_{j+1/2})$ are the slope limiters which are functions of adjacent discrete gradients

$$\mathbf{r}^+_{j+1/2} = \frac{\mathbf{S}_j - \mathbf{S}_{j-1}}{\mathbf{S}_{j+1} - \mathbf{S}_j}, \quad \mathbf{r}^-_{j+1/2} = \frac{\mathbf{S}_{j+2} - \mathbf{S}_{j+1}}{\mathbf{S}_{j+1} - \mathbf{S}_j}. \tag{21}$$

5.1.2 Primitive variables

Writing the scheme using the primitive variables gives

$$\mathbf{S}_L = \mathbf{S}_j + \frac{1}{2}\mathbf{P}\Phi(\mathbf{r}^+_{j+1/2})(\mathbf{C}_{j+1} - \mathbf{C}_j) \tag{22}$$

$$\mathbf{S}_R = \mathbf{S}_{j+1} - \frac{1}{2}\mathbf{P}\Phi(\mathbf{r}^-_{j+1/2})(\mathbf{C}_{j+1} - \mathbf{C}_j) \tag{23}$$

where $\mathbf{P}$ denotes the transformation matrix between conservative and primitive variables. The slope limiters $\Phi(r^{\pm}_{j+1/2})$ are functions of

$$\mathbf{r}^+_{j+1/2} = \frac{\mathbf{C}_j - \mathbf{C}_{j-1}}{\mathbf{C}_{j+1} - \mathbf{C}_j}, \quad \mathbf{r}^-_{j+1/2} = \frac{\mathbf{C}_{j+2} - \mathbf{C}_{j+1}}{\mathbf{C}_{j+1} - \mathbf{C}_j}. \tag{24}$$

5.2 Monotonicity

Both the Minmod and the Superbee limiters[20] are used in this paper. The Fromm limiter which is precisely Van Leer's original limiter [13] is defined by

$$\Phi_{Fromm}(r) = \max(0, \min(2r, 2, \frac{1+r}{2})). \tag{25}$$

which has been proven to be the most reliable.

5.3 Incorporating the monotone numerical flux

Then, the Rusanov flux described in (17) is applied to the higher order data so that the Riemann problem is resolved with a higher order flux of the form

$$\mathbf{f}_{j+1/2} = \frac{1}{2}[(\mathbf{f}(\mathbf{S}_L) + \mathbf{f}(\mathbf{S}_R)) - \mid \Lambda_{RUj+1/2} \mid (\mathbf{S}_R - \mathbf{S}_L)]. \tag{26}$$

5.4 Time Stepping

The semi discrete formulation of the scheme is written as

$$\frac{d}{dt}\mathbf{S}_j = -\frac{1}{\Delta x}[\mathbf{f}_{j+1/2} - \mathbf{f}_{j-1/2}] \tag{27}$$

and is finally integrated using monotonicity preserving Runge Kutta method described in section 6.3.

6 FORMULATION OF A NON UPWIND RKDG METHOD

In this section, the RKDG method is briefly introduced for the one dimensional scalar conservation law. Systems are approximated component by component, except for the limiting step where the primitive variables are chosen instead of the conservative ones.

6.1 The DG Space Discretisation

In finite element methods, the approximate solution S_h is chosen to belong to a finite-dimensional space V_h. Its degrees of freedom are then obtained by solving a weak formulation of (6) that is usually obtained by multiplying (6) by a test function $v_h \in V_h$, integrating over suitable domains, and finally integrating by parts. The finite element used here is a Galerkin method for which

$$V_h = \{p \in BV(\Omega) \cap L^1(\Omega) : p_{|I_j} \in P^k(I_j)\}; \tag{28}$$

where $P^k(I_j)$ is the space of polynomials in I_j of degree at most k on I_j and BV the space of functions with bounded variation. Note that in V_h, the functions are allowed to have jumps at the interfaces $x_{j+1/2}$. This is one of the main differences between the discontinuous Galerkin method and most of the finite element methods.

6.1.1 Weak formulation

Multiplying equation (6) by arbitrary smooth functions v and integrating over I_j gives after integration by part:

$$\begin{aligned} \int_{I_j} \partial S_t(x,t)v(x)dx &= \int_{I_j} f(S(x,t))\partial_x v(x)dx \\ &\quad -(f(S(x_{j+1/2},t))v(x^-_{j+1/2}) - f(S(x_{j-1/2},t))v(x^+_{j-1/2})), \end{aligned} \tag{29}$$

Next v is replaced by a test functions in V_h, and the exact solution by the approximate solution S_h.

6.1.2 Data reconstruction and basis functions

Let $\{\Psi^l_j; l = 0..k\}$ be the basis of Legendre polynomials on I_j. The choice of using Legendre Polynomials stems from their properties to constitute a local L^2-orthogonal basis over I_j, which gives a diagonal mass matrix in the 1-D case.
The approximate solution can be written as

$$S_h(x,t)_{|I_j} = \sum_{l=0}^{l=k} S^l_j(t)\Psi^l_j(x), \tag{30}$$

where $\{S_j{}^l\}^{l=k}_{l=0}$ denote the degrees of freedom of S_h in the interval I_j. Taking $v_h = \Psi^l_j$ and using the orthogonality property of Ψ^l_j yields:

$$\int_{I_j} \Psi_j^l(x)^2 dx \frac{dS_j^l}{dt} = \int_{I_j} f(S_h(x,t))\partial_x \Psi_j^l(x) dx - [f_{j+1/2}(t)\Psi_j^l(x_{j+1/2}) - f_{j-1/2}(t)\Psi_j^l(x_{j-1/2})]. \quad (31)$$

On the other hand, choosing $\Psi_j^l(x) = P_l(2(x-x_j)/\Delta x_j)$, where P_l denote the Legendre polynomial of degree l on $(-1,1)$, we obtain

$$\int_{I_j} \Psi_j^l(x)^2 dx = \frac{\Delta x_j}{2l+1}, \quad \Psi_j^l(x_{j+1/2}) = 1, \quad \Psi_j^l(x_{j-1/2}) = (-1)^l. \quad (32)$$

The DG space discretisation of (6) reduces to an *independent* system of ODEs for the degrees of freedom that can be written in the form:

$$\frac{d}{dt} S_j^l = \mathcal{L}_j^l(S_{h|I_j}) \quad (33)$$

where

$$\mathcal{L}_j^l = \frac{1}{\Delta x_j} \int_{I_j} f(S_h(x,t))\partial_x \Psi_j^l(x) dx - \frac{1}{\Delta x_j}[f_{j+1/2}(t) - (-1)^l f_{j-1/2}(t))]. \quad (34)$$

Here the local discrete operator $\mathcal{L}_j^l$ approximates $-f(S)_x$ on I_j. Notice the local property of this formulation which renders the method highly parallelizable.

6.1.3 Stabilization by local projection limiting

In order to achieve local maximum principle with respect to the means, the reconstructed values at the interfaces $S_{j+1/2}^{\pm}$ need to be modified by some local projection limiter. Indeed, writing

$$S_{j+1/2}^- = \bar{S}_j + \tilde{S}_j \quad (35)$$

$$S_{j+1/2}^+ = \bar{S}_{j+1} - \tilde{\tilde{S}}_{j+1}, \quad (36)$$

the scheme for the means $\bar{S}_j = \frac{1}{\Delta x}\int_{I_j} S_h(x)dx$ reduces to a semi discrete finite volume form

$$\frac{d}{dt}\bar{S}_j = -\frac{1}{\Delta x_j}[f_{j+1/2} - f_{j-1/2}]. \quad (37)$$

Discontinuous Galerkin methods can be interpreted as a generalization of the finite volume methods to higher order accuracy via a finite element based data reconstruction operator $R_k^0 : V_h^0 \to V_h^k$, $R_k^0 \bar{S} = S_h$.

Recalling the Legendre polynomials orthogonality properties and that $\int_{I_j} \Psi_j^l(x)dx = 0$ for $l \geq 1$, we have

$$\bar{S}_j = S_j^0, \quad \tilde{S}_j = \sum_{l=1}^{l=k} S_j^l(t), \quad \tilde{\tilde{S}}_j = -\sum_{l=1}^{l=k} (-1)^l S_j^l(t). \quad (38)$$

Next, the high order data is limited via the use of the restrictive limiter

$$\Lambda\Pi_{\frac{1}{2}} S^-_{j+1/2} = \bar{S}_j + m(\tilde{S}_j, \frac{1}{2}\Delta_+\bar{S}_j, \frac{1}{2}\Delta_-\bar{S}_j) \quad (39)$$

$$\Lambda\Pi_{\frac{1}{2}} S^+_{j+1/2} = \bar{S}_{j+1} - m(\tilde{\bar{S}}_{j+1}, \frac{1}{2}\Delta_+\bar{S}_{j+1}, \frac{1}{2}\Delta_-\bar{S}_{j+1}) \quad (40)$$

and the less restrictive limiter proposed by Cockburn[4]

$$\Lambda\Pi_1 S^-_{j+1/2} = \bar{S}_j + m(\tilde{S}_j, \Delta_+\bar{S}_j, \Delta_-\bar{S}_j) \quad (41)$$

$$\Lambda\Pi_1 S^+_{j+1/2} = \bar{S}_{j+1} - m(\tilde{\bar{S}}_{j+1}, \Delta_+\bar{S}_{j+1}, \Delta_-\bar{S}_{j+1}) \quad (42)$$

This limiter corresponds to adding the minimum amount of numerical diffusion while preserving the stability of the scheme. The DG method combined with the slope limiters stated above is proven to be stable[19].

In an attempt to reproduce an equivalent to the Fromm limiter described in (25), the following Fromm type limiter is introduced for the DG method:

$$\Lambda\Pi_{Fromm} S^-_{j+1/2} = \bar{S}_j + m(\min(\tilde{S}_j, \frac{\bar{S}_{j+1} - \bar{S}_{j-1}}{4}), \Delta_+\bar{S}_j, \Delta_-\bar{S}_j) \quad (43)$$

$$\Lambda\Pi_{Fromm} S^+_{j+1/2} = \bar{S}_{j+1} - m(\min(\tilde{\bar{S}}_{j+1}, \frac{\bar{S}_{j+2} - \bar{S}_j}{4}), \Delta_+\bar{S}_{j+1}, \Delta_-\bar{S}_{j+1}) \quad (44)$$

6.1.4 System of hyperbolic equations

Systems are approximated component by component, except for the limiting step where either the conservative or the primitive variables are chosen. In the case, where the limiting affects the primitive variables, Eq's.(41, 39) take respectively the forms

$$\Lambda\Pi_1 \mathbf{S}^-_{j+1/2} = \bar{\mathbf{S}}_j + \mathbf{P}m(\tilde{\mathbf{C}}_j, \Delta_+\bar{\mathbf{C}}_j, \Delta_-\bar{\mathbf{C}}_j) \quad (45)$$

$$\Lambda\Pi_1 \mathbf{S}^+_{j+1/2} = \bar{\mathbf{S}}_{j+1} - \mathbf{P}m(\tilde{\bar{\mathbf{C}}}_{j+1}, \Delta_+\bar{\mathbf{C}}_{j+1}, \Delta_-\bar{\mathbf{C}}_{j+1}) \quad (46)$$

and

$$\Lambda\Pi_{\frac{1}{2}} \mathbf{S}^-_{j+1/2} = \bar{\mathbf{S}}_j + \mathbf{P}m(\tilde{\mathbf{C}}_j, \frac{1}{2}\Delta_+\bar{\mathbf{C}}_j, \frac{1}{2}\Delta_-\bar{\mathbf{C}}_j) \quad (47)$$

$$\Lambda\Pi_{\frac{1}{2}} \mathbf{S}^+_{j+1/2} = \bar{\mathbf{S}}_{j+1} - \mathbf{P}m(\tilde{\bar{\mathbf{C}}}_{j+1}, \frac{1}{2}\Delta_+\bar{\mathbf{C}}_{j+1}, \frac{1}{2}\Delta_-\bar{\mathbf{C}}_{j+1}) \quad (48)$$

and Eq. (43) writes

$$\Lambda\Pi_{Fromm} \mathbf{S}^-_{j+1/2} = \bar{\mathbf{S}}_j + \mathbf{P}m(\min(\tilde{\mathbf{C}}_j, \frac{\bar{\mathbf{C}}_{j+1} - \bar{\mathbf{C}}_{j-1}}{4}), \Delta_+\bar{\mathbf{C}}_j, \Delta_-\bar{u}_j) \quad (49)$$

$$\Lambda\Pi_{Fromm} \mathbf{S}^+_{j+1/2} = \bar{\mathbf{S}}_{j+1} - \mathbf{P}m(\min(\tilde{\bar{\mathbf{C}}}_{j+1}, \frac{\bar{\mathbf{C}}_{j+2} - \bar{\mathbf{C}}_j}{4})), \Delta_+\bar{\mathbf{C}}_{j+1}, \Delta_-\bar{\mathbf{C}}_{j+1}) \quad (50)$$

where $\mathbf{P}$ is the transformation matrix between conservative $\mathbf{S}$ and primitive variables $\mathbf{C}$.

6.2 Incorporating the monotone numerical flux

The discrete approximation is discontinuous at the cell interface $x_{j+1/2}$ and the non-linear flux $f(S(x_{j+1/2}))$ is approximated by a *numerical flux* h that depends on the two values of S_h at each side of the interface i.e.

$$f_{j+1/2}(t) = h(S(x^-_{j+1/2}, t), S(x^+_{j+1/2}, t)). \tag{51}$$

The numerical flux is assumed to be *locally lipschitz continuous* and satisfies the *conservation* property, the *consistency* property which is obtained if the numerical flux with identical state arguments reduces to the true flux of the same state and the *monotone* property, which ensures that the scheme converges to the entropy satisfying weak solution. In this work, Rusanov flux (15) is selected.

6.3 Rung Kutta time discretisation

To discretize the system of ODEs (33), higher-order Runge Kutta time discretizations are used. As shown by Cockburn[4], when polynomials of degree k are used, a Runge Kutta method of order $k+1$ must be used in order to guarantee that the scheme is stable. The Runge Kutta time discretization introduced in[7] is used to integrate the ODE system (33) in time.

The resulting RKDG method with the slope limiter previously described is proven to be TVDM (Total Variation Diminishing in the Means) for a scalar equation.
Further details of the method can be found in [3,4,5].

7 NUMERICAL RESULTS in 1D

7.1 Two phase flow

In the case of water-oil two phase flow, both Buckley Leverett with and without gravity fluxes have been implemented. Quadratic mobilities have been considered and the mobility ratio is set to 1.

For the Buckley Leverett case zero gravity, water is continuously injected at the left hand boundary and fluid is produced at the right hand side boundary. The computed and exact water saturation are shown in figures 1-4 at time 0.5 with the prescribed initial conditions $S = 1, x = 0$ and $S = 0, x > 0$.

For the gravity segregation with reverse flow, the computed and exact water saturation are shown in figures 5-8 at time 1.25 with the prescribed initial conditions initial conditions are $S = 1, x >= 0.5$ and $S = 0, x < 0.5$.

All the results shown have been produced on a grid of 100 nodes.

The second order numerical results using the non upwind high order schemes are displayed in Figure 3 and are very similar to those obtained using the upwind flux described by equations (8), (9) for the Buckley Leverett case, as displayed in Figure 4.

Resolution near the shocks is improved using nonupwind DG and MUSCL schemes combined with the minmod limiter (Figures 2, 6) comparatively to the first order results

(Figures 1, 5) as the numerical diffusion near the shock is noticeably reduced. Both DG and MUSCL using linear reconstructions show similar resolution when the minmod limiter is used.

The DG shows better overall resolution when using the Fromm limiter (Figures 3, 7).

7.2 Three component two-phase flow

The schemes are compared for gravity segregation with reverse flow. Initial data consists of a vertical aqueous phase column above an oil column of equal volume (95% oil saturation), separated by a diaphragm which is removed at time $t = 0$. The heavier miscible phase moves downwards, creating a shock followed by a constant state, contact discontinuity due to the polymer and rarefaction wave. The oil moves upwards creating a shock at the opposite end of the rarefaction. Quadratic relative permeabilities are assumed and the normalised aqueous viscosity is a function of polymer concentration. The computed and exact water saturation are shown in figures 9-15 at time 1.25, with the prescribed initial date

$$\begin{cases} S, C = 0.05, 0.1, & x \leq 0.5; \\ S, C = 1.0, 07, & \text{otherwise.} \end{cases} \tag{52}$$

The contact discontinuity caused by the linearly degenerate polymer component is particularly difficult to capture numerically as it is not self sharpening. The saturation and polymer concentration profiles are heavily smeared by the first order Godunov scheme scheme (Figure 8), demonstrating that the large amount of numerical diffusion present in the low-order scheme and rendering it unable to cope with the rarefaction and the contact discontinuity caused by the polymer. In contrast, excellent resolution of the rarefaction and shock are obtained by both the DG scheme (Figure 9) with similar resolution to the higher order MUSCL scheme (Figure 10) using the minmod limiter (most smearing) applied to the primitive variables for both cases.

A componentwise formulation using conservative variable reconstruction fails to preserve the monotonicity of the solution as both schemes yield oscillatory solution near as displayed in figures 11 and 12. In contrast, the primitive variable reconstruction schemes (DG and MUSCL) are oscillation free, with the Fromm limiter giving sharper and monotone profiles. The higher order MUSCL scheme yields a sharper contact discontinuity using the Fromm limiter. However, our results for three component two phase flow are found to be over compressive when the least restrictive limiter, ($\Lambda\Pi_1$) is used for the DG, and accordingly the superbee limiter is applied to the high order MUSCL data.

8 Conclusions

A novel non upwind discontinuous galerkin method is presented for hyperbolic conservation laws in reservoir simulation. The scheme has the following properties:

1. upwind and characteristic decomposition are circumvented, leading to a fundamental simplification of current methods.

2. Higher order accuracy is achieved in space and time.

3. Local conservation is maintained.

Results are presented for gravity driven flows involving two phase flow and three component two phase flow, where the wave direction changes sign (reverse flow) in one dimension. A new DG limiter is presented which gives the best results in tests to date. Both the MUSCL Godunov finite volume method and the DG method with linear constructions yield similar accuracy for the same type of limiter. Both schemes are more accurate and efficient compared to first order method. However, As the degrees of freedom for the DG method are twice larger than for the Godunov method in the case of linear rconstruction, the MUSCL finite volume method shows better efficiency than DG method for the examples presented. However DG methods may be more appropriate for very high order or multidimensional approximations.

Finally, this work emphases the importance of using primitive variables and choice of limiter for nonupwind DG methods in order to preserve the monotonicity without destroying high order accuracy.

9 ACKNOWLEDGEMENT

First author is supported by the EPSRC grant GR/S70968/01. Second author is supported in part by the same grant.

REFERENCES

[1] A.Burbeau, P.Sagaut and Ch.-H. Bruneau *A problem-Indpendent Limiter for High-Order Runge Kutta Discontinuous Galerkin Methods*, *Journal of Computational Physics* , Vol. 169., (1989), Vol. II., (1991).

[2] S.Idelsohn and E.Oñate. Finite element and finite volumes. Two good friends. *Int. J. Num. Meth. Engng.*, **37**, 3323–3341, (1994).

[3] B.Cockburn and C.W.Shu. *TVB Runge-Kutta Local Projection Discontinuous Galerkin Method for Conservation Laws II: General Framework Mathematics of Computation*, **52**, 411–435, (1989).

[4] B.Cockburn. *Discontinuous Galerkin Methods for convection-dominated problems Higher Order Methods for Computational Physics*, Lecture Notes in Computational Science and Engineering **9**, 69–224, (1999).

[5] B.Cockburn and S.Y.Lin. *TVB Runge-Kutta Local Projection Discontinuous Galerkin Method for Conservation Laws III: One Dimensional sytems Journal of Computational Physics*, **84**, 90–113, (1989).

[6] A.Burbeau, P.Sagaut and Ch.-H. Bruneau. *A problem-Indpendent Limiter for High-Order Runge Kutta Discontinuous Galerkin Methods Journal of Computational Physics*, **169**, 111–150, (2001).

[7] B.Gottlieb and C.W. Shu. *Total Variation Diminishing Runge Kutta Schemes Mathematics of Computation*, **67**, 73–85, (1998).

[8] H.Hoteit, Ph.Ackerer, R.Mosé, J.Erhel and B. Philippe. *New Two Dimensional slope limiters for discontinuous Galerkin method on arbitrary meshes International Journal for Numerical Methods in Engineering*, **61**, 2566–2593, (2004).

[9] S.Osher, S.Chakravarthy. *High Resolution schemes and the entropy condition SIAM Journal on Numerical Analysis*, **21**, 955–984, (2004).

[10] E.Godlewski and P.Raviart. Numerical Approximation of Hyperbolic Systems of Conservation Laws. *Applied Mathematical Science 118*, (1996).

[11] V.V Rusanov. *Calculation of interaction of non steady shock waves with obstacles Journal of Computational Physics*, **USSR1** 267-279, (1961).

[12] X.D.Liu, S.Osher. *Conevx ENO High Order Multidimensional Schemes Without Field by Field Decomposition on staggered grids Journal of Comuptational Physics*, **141**, 1–27, (1998).

[13] B. Van Leer. *Towards the Ultimate Conservative Difference Scheme V. A Second Order Sequel to Godunov's Method Journal of Comuptational Physics*, **32**, 101–136, (1979).

[14] K. Aziz and A. Settari. Petroleum Reservoir simulation *Applied Science Publishers*, (1979).

[15] J.B.Bell, P.Collela and J.A.Trangenstein *Higher Order Godunov Methods for general systems of hyperbolic conservation laws Journal of Comuptational Physics*, **82**, 362–397, (1989).

[16] M.G.Edwards *A Higher Order Godunov Scheme Coupled With Dynamic Local Grid Refinement for Flow In a Porous Medium Computational Methods Applied Mechanical Engineering*, **131**, 287–308, (1996).

[17] H.Hoteit and A.Firoozabadi *Compositional Modeling by the Combined Discontinuous Galerkin and Mixed Methods SPE*, **11**, 19–34, (2006).

[18] M.G.Edwards *Non upwind Versus Upwind Schemes for Hyperbolic conservation Laws SPE*, **93691-MS**, (2005).

[19] V.Gowda, J.A.Jaffr *A discontinuous finite element method for scalar nonlinear conservation laws. Rapport de recherche INRIA* **1848**, (1993).

[20] P. K. Sweby *High Resolution Schemes Using Flux Limiters for Hyperbolic Conservation Laws. SIAM Journal on Numerical Analysis* **21**, 995–1011, (1984).

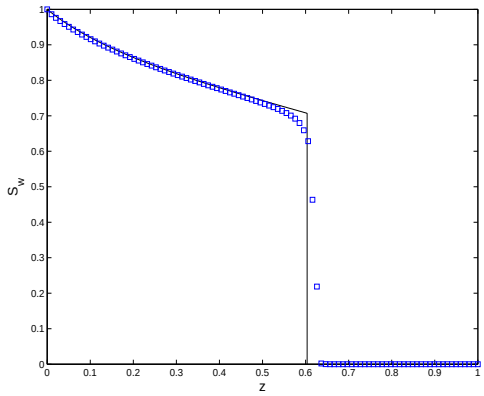

(a)

Figure 1: Buckley Leverett problem with non-upwind Rusanov flux. First Order results.

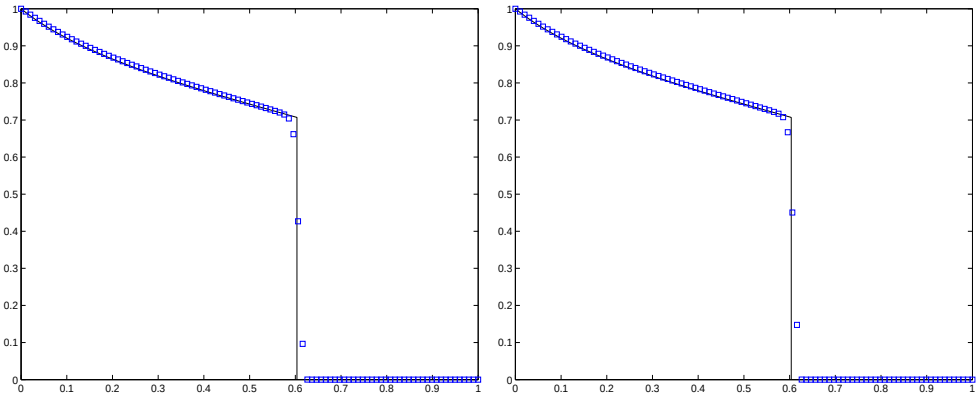

(a) (b)

Figure 2: P1 results with the minmod limiter and Rusanov non upwind flux for the Buckley Leverett equation. (a) Discontinuous Galerkin formulation (b) MUSCL formulation

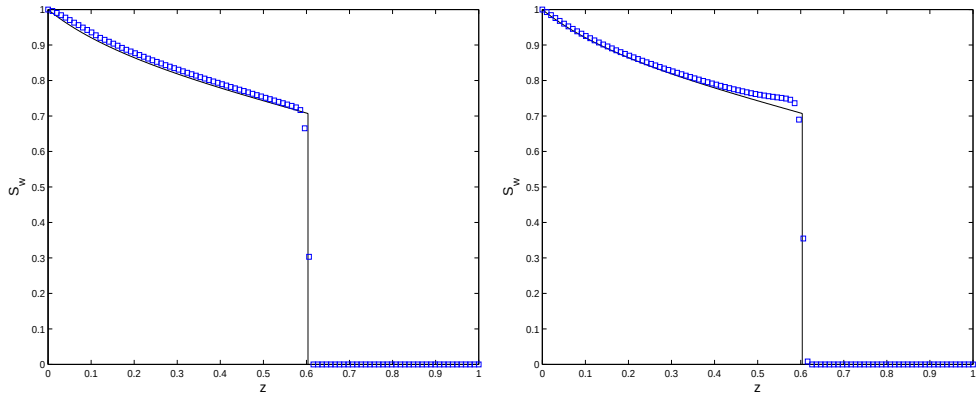

(a) (b)

Figure 3: P1 results with the Fromm type limiter and Rusanov non upwind flux for the Buckley Leverett equation. (a) Discontinuous Galerkin formulation (b) MUSCL formulation

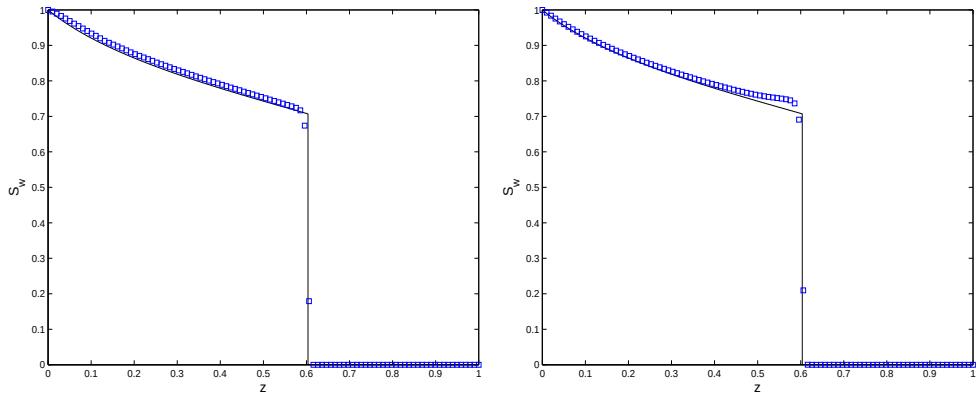

(a) (b)

Figure 4: P1 results with the Fromm limiter and the upwind flux for the Buckley Leverett equation. (a) Discontinuous Galerkin formulation (b) MUSCL formulation

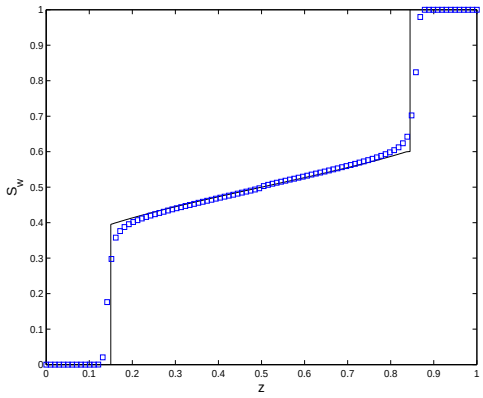

(a)

Figure 5: Gravity driven two phase flow with non-upwind Rusanov flux. First Order results.

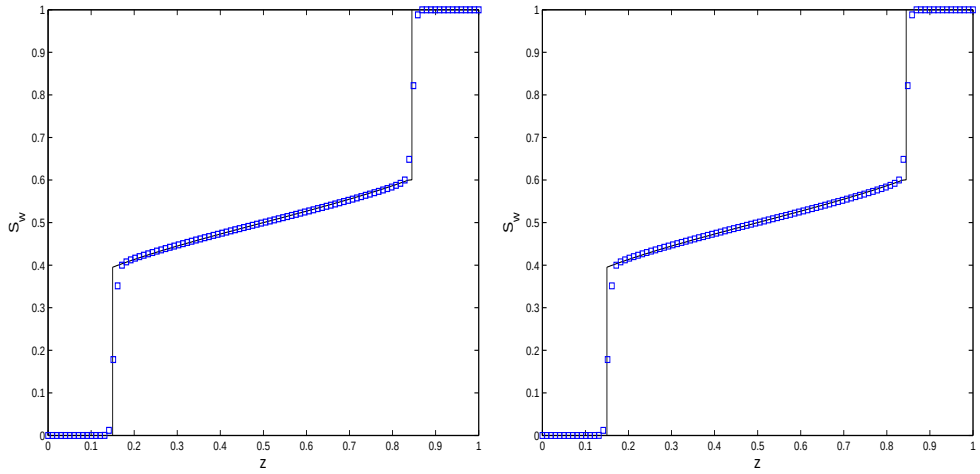

(a) (b)

Figure 6: P1 results with the minmod limiter and Rusanov non upwind flux for the gravity driven two phase flow. (a) Discontinuous Galerkin formulation (b) MUSCL formulation

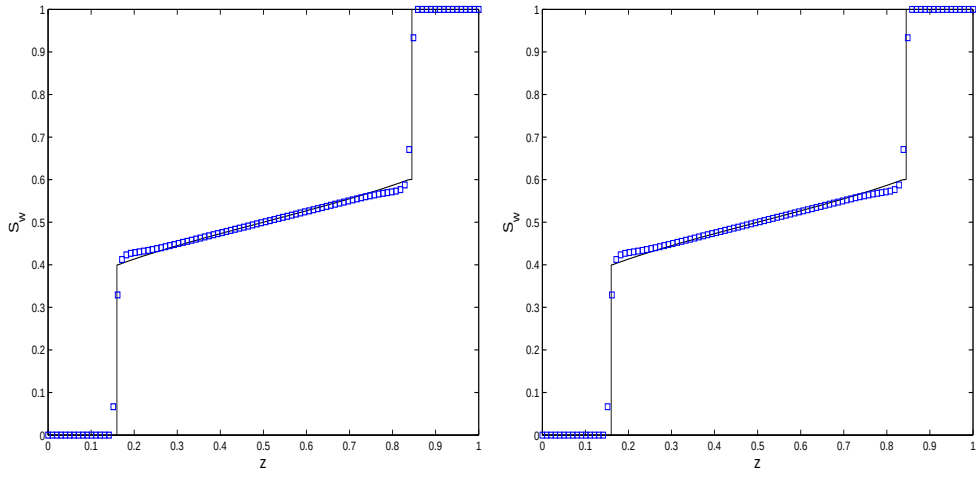

(a) (b)

Figure 7: P1 results with the Fromm type limiter and Rusanov non upwind flux for the gravity driven two phase flow. (a) Discontinuous Galerkin formulation (b) MUSCL formulation

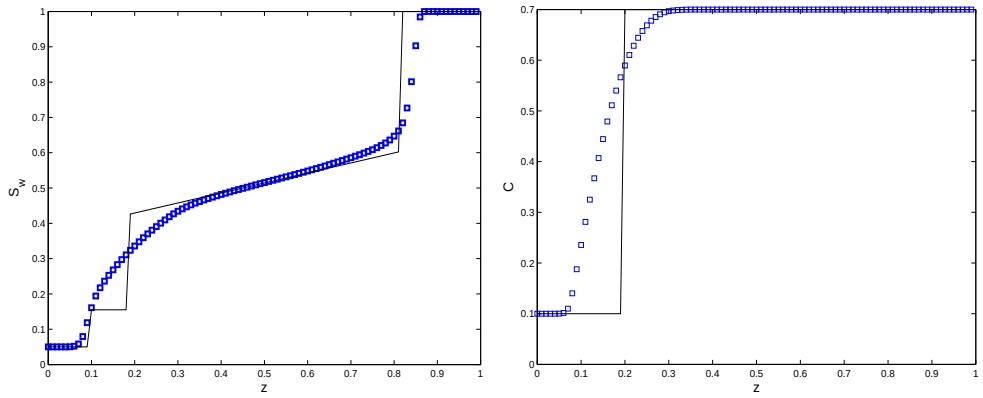

(a) (b)

Figure 8: Gravity driven three component two phase flow with non-upwind Rusanov flux. First Order.

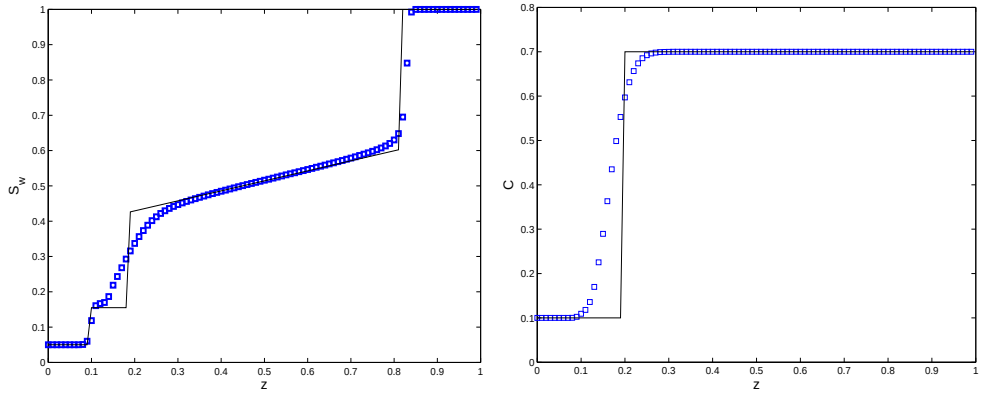

(a) (b)

Figure 9: P1 Discontinuous Galerkin results with the minmod limiter applied to the primitive variables and Rusanov non upwind flux for the gravity driven two phase flow. (a) Aqueous saturation (b) Polymer concentration

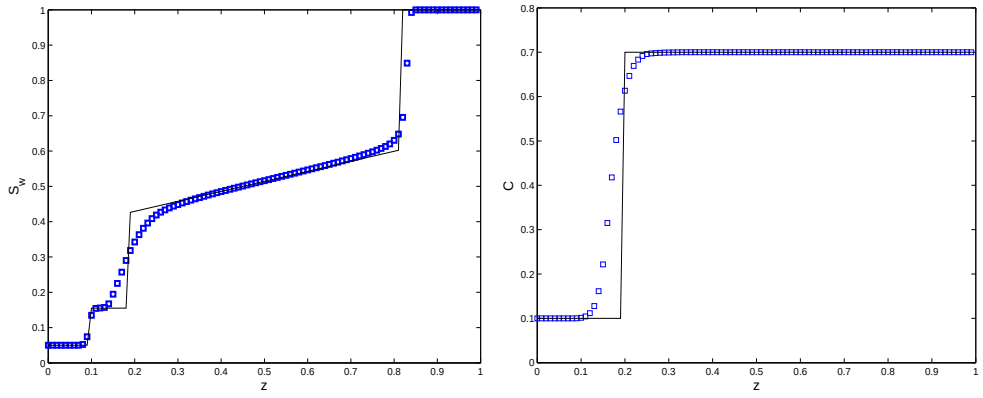

(a) (b)

Figure 10: P1 MUSCL results with the minmod limiter applied to the primitive variables and Rusanov non upwind flux for the gravity driven two phase flow. (a) Aqueous saturation (b) Polymer concentration

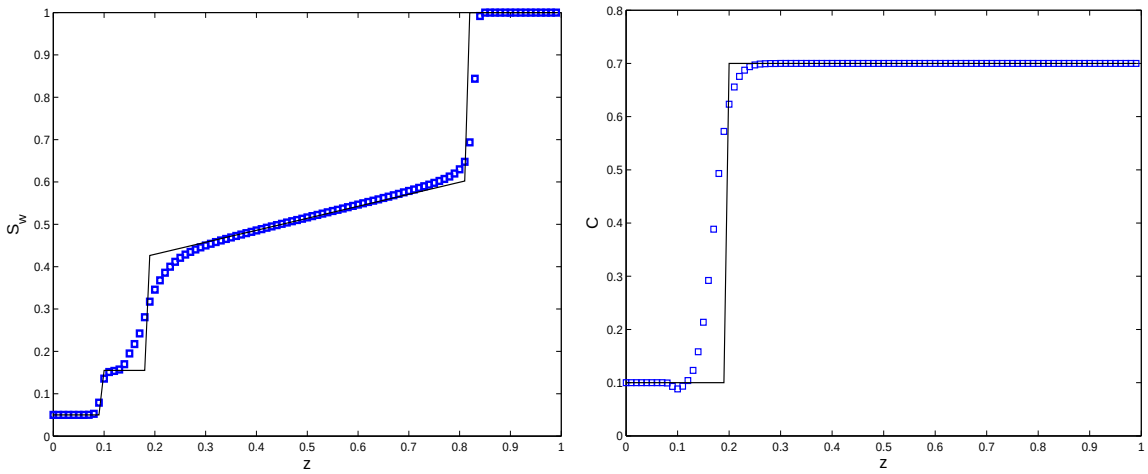

(a) (b)

Figure 11: P1 Discontinuous Galerkin results with the minmod limiter applied to the conservative variables and Rusanov non upwind flux for the gravity driven two phase flow. (a) Aqueous saturation (b) Polymer concentration

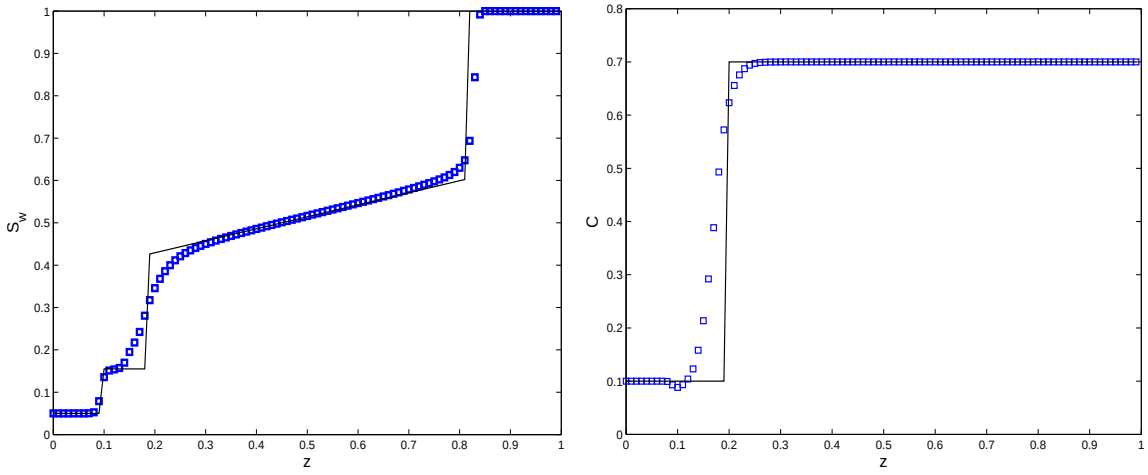

(a) (b)

Figure 12: P1 MUSCL results with the minmod limiter applied to the conservative variables and Rusanov non upwind flux for the gravity driven two phase flow. (a) Aqueous saturation (b) Polymer concentration

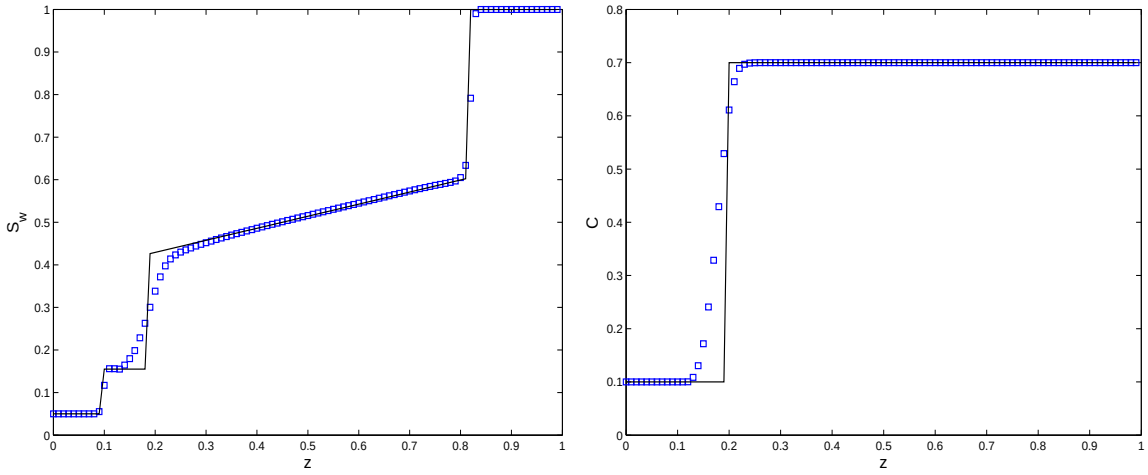

(a) (b)

Figure 13: P1 Discontinuous Galerkin results with the Fromm type limiter applied to the primitive variables and Rusanov non upwind flux for the gravity driven two phase flow. (a) Aqueous saturation (b) Polymer concentration

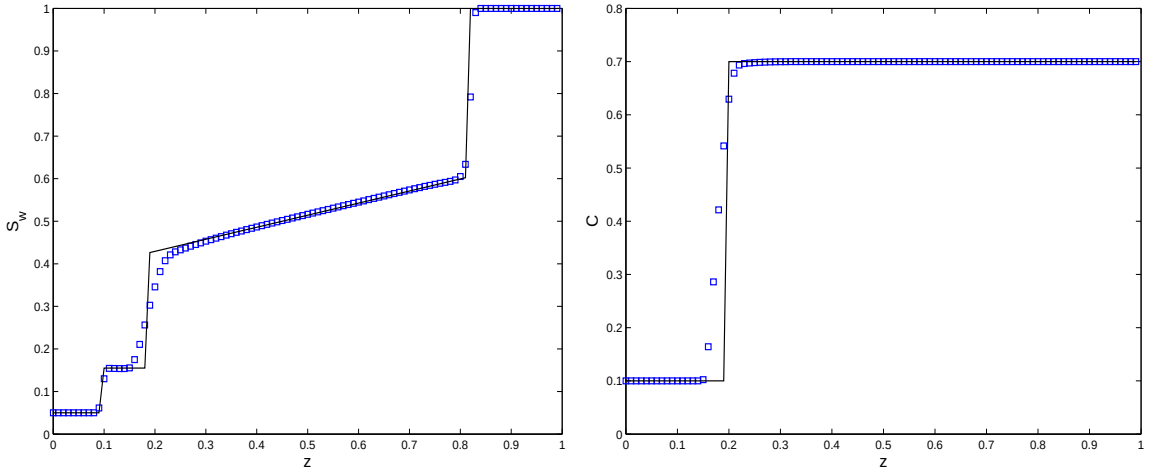

(a) (b)

Figure 14: P1 MUSCL results with the Fromm type limiter applied to the primitive variables and Rusanov non upwind flux for the gravity driven two phase flow. (a) Aqueous saturation (b) Polymer concentration